

УДК 539.17 + 539.172.16

SOME PECULIARITIES IN THE INTERACTION OF ${}^6\text{He}$ WITH ${}^{197}\text{Au}$ AND ${}^{206}\text{Pb}$

*Yu. E. Penionzhkevich^a, R. A. Astabatyanyan^a, N. A. Demekhina^b, Z. Dlouhy^c,
R. Kalpakchieva^a, A. A. Kulko^a, S. P. Lobastov^a, S. M. Lukyanov^a,
E. R. Markaryan^a, V. A. Maslov^a, Yu. A. Muzychka^a, Yu. Ts. Oganessian^a,
D. N. Rassadov^a, N. K. Skobelev^a, Yu. G. Sobolev^a, V. Yu. Ugryumov^c,
J. Vincour^c, T. Zholdybaev^d*

^aJoint Institute for Nuclear Research, Dubna

^bYerevan Physics Institute, Yerevan, Armenia

^cInstitute of Nuclear Physics, Rez near Prague, Czech Republic

^dInstitute of Nuclear Physics, Almaty-82, Kazakhstan

Excitation functions were measured for fusion followed by the evaporation of neutrons in the reactions ${}^{206}\text{Pb}({}^6\text{He}, 2n){}^{210}\text{Po}$ and ${}^{197}\text{Au}({}^6\text{He}, xn){}^{203-xn}\text{Tl}$, where $x = 2-7$, as well as for the transfer reactions on a ${}^{197}\text{Au}$ target with the formation of the ${}^{196}\text{Au}$, ${}^{198}\text{Au}$ and ${}^{199}\text{Au}$ isotopes. The experiment was carried out at the Dubna Radioactive Ion Beams (DRIBs) complex of FLNR, JINR. The ${}^6\text{He}$ beam intensity was about $5 \cdot 10^6$ pps, the maximum energy being (60.3 ± 0.4) MeV. A significant increase in the cross section was observed below the Coulomb barrier for the fusion reaction with the evaporation of two neutrons compared to statistical model calculations. Unusual behaviour for the production of ${}^{198}\text{Au}$ is observed, whereas the cross section for the formation of ${}^{199}\text{Au}$ is very low. The analysis of the data in the framework of the statistical model for the decay of excited nuclei, which took into account the sequential fusion of ${}^6\text{He}$, has shown good agreement between the experimental and calculated values of the cross sections for the case of sub-Coulomb-barrier fusion in the ${}^{206}\text{Pb} + {}^6\text{He}$ reaction.

Представлены экспериментально измеренные функции возбуждения для каналов слияния с последующим испарением нейтронов ${}^{206}\text{Pb}({}^6\text{He}, 2n){}^{210}\text{Po}$ и ${}^{197}\text{Au}({}^6\text{He}, xn){}^{203-xn}\text{Tl}$, где $x = 2-7$, а также для реакций передачи на ${}^{197}\text{Au}$ с образованием изотопов ${}^{196}\text{Au}$, ${}^{198}\text{Au}$ и ${}^{199}\text{Au}$. Эксперимент проводился на ускорительном комплексе радиоактивных пучков DRIBs (ОИЯИ). Интенсивность пучка ${}^6\text{He}$ составляла $5 \cdot 10^6 \text{ с}^{-1}$, максимальная энергия $(60,3 \pm 0,4)$ МэВ. Наблюдалось значительное увеличение сечения канала реакции слияния с испарением двух нейтронов в подбарьерной области энергий по сравнению с расчетами по статистической модели. Наблюдалось необычное поведение образования изотопа ${}^{198}\text{Au}$, а также относительно малое сечение образования изотопа ${}^{199}\text{Au}$. Проведенный анализ экспериментальных данных в рамках статистической модели распада возбужденных ядер с учетом последовательного слияния ядра ${}^6\text{He}$ показал хорошее согласие экспериментальных и расчетных значений сечения для подбарьерного слияния ядер в реакции ${}^{206}\text{Pb} + {}^6\text{He}$.

INTRODUCTION

The interaction of halo nuclei with other nuclei for almost 10 years now has been of increased interest from experimental and theoretical point of view. Still much attention is paid to ${}^6\text{He}$ -induced reactions leading to the formation of a compound nucleus followed by the evaporation of neutrons or fission. The particular interest to this type of investigations arose

when in 1995 in Ref. [1], which was dedicated to the study of fission of the compound nucleus ${}^{215}\text{At}$, formed in the bombardment of a ${}^{209}\text{Bi}$ target with ${}^6\text{He}$ ions, a significant enhancement was observed in the cross section, especially in the sub-Coulomb barrier, compared to the expected according to the statistical model. Such an enhancement was earlier predicted in a series of theoretical papers [2, 3]. In particular, an increase of the probability of penetrating (tunneling) through the potential barrier due to its extended neutron distribution, compared to that in ordinary nuclei close to the line of stability, was predicted for ${}^{11}\text{Li}$. Such distributions, as has been shown in Ref. [4], may bring forth a coupling of the collective degrees of freedom and, respectively, an increase of the reaction cross section, especially in the subbarrier region. The extended distribution of nuclear matter is characteristic for light neutron-rich nuclei, in which the presence of valence neutrons can lead to the formation of a neutron halo. ${}^6\text{He}$ and ${}^{11}\text{Li}$ are among the nuclei with such a structure. On the other hand, such nuclei are weakly bound, which, in turn, leads to an increase in the probability of their breakup that may be accompanied by the consequent fusion of the residual nucleus (the core) with the target nucleus or by the transfer of nucleons without any further interaction between the nuclei. The variety of possible processes makes it difficult to analyze the experimental data and requires the consideration of all possible reaction channels.

Soon after the first experimental paper on the fusion–fission reaction induced by ${}^6\text{He}$ [1], a series of experiments was undertaken, whose aim was to determine the probability of fusion of ${}^6\text{He}$ with other nuclei close to the Coulomb barrier. For instance, in [5] Kolata et al. investigated the same reaction, ${}^{209}\text{Bi} + {}^6\text{He}$, as was used in [1]. The excitation functions for the decay of the compound nucleus by emission of three neutrons were measured and the comparison with the statistical model for the formation and decay of the compound nucleus confirmed that an enhancement of subbarrier fusion of ${}^6\text{He}$ nuclei takes place. The next measurement of the excitation function for the fission channel in the ${}^6\text{He} + {}^{238}\text{U}$ reaction [6] also allowed one to draw a conclusion that the probability of fusion–fission, when using a ${}^6\text{He}$ beam at Coulomb barrier energies, is strongly enhanced. However, a later experiment of the same group involving the measurement of the fission fragments in coincidence with α particles, produced after the breakup of ${}^6\text{He}$, has shown that subbarrier fusion–fission for this reaction can easily be explained in terms of the fission of the uranium target after the transfer of one or two neutrons. As a result, these authors [6] came out with the new paper [7], in which they insist that in the mentioned reaction enhancement of the fusion of ${}^6\text{He}$ is not observed. There are a few more papers reporting on fusion reactions with ${}^6\text{He}$ [8, 9]. However, these measurements require the inclusion of more information on the different exit channels and higher statistics in order to be considerably more reliable. The existence of such controversial data is evidence of the difficulties which have to be overcome in experiments with radioactive ion beams. One such a problem, in the first place, is the low intensity of the secondary beams. This makes measurements in the region of the Coulomb barrier extremely time-consuming, if high statistics is to be obtained. Secondly, in order to study the excitation functions in a broad energy range (5–70 MeV/A), it is necessary to decrease the beam energy using degraders, which in turn deteriorates the beam energy dispersion. Finally, at the relatively low beam intensity it is desirable to use detector arrays of high efficiency, located at forward angles with respect to the beam direction. All this was taken into account when preparing the experiments described below.

The launching of the accelerator complex for radioactive beams DRIBs [10] at FLNR (JINR) at the end of 2004 made it possible to produce ${}^6\text{He}$ beams with an intensity of up to

$5 \cdot 10^6$ pps in a wide range of energies (3–10 MeV/A) with an energy resolution not worse than 1%. It is necessary to note that such conditions can be provided only at facilities based on the ISOL-method. Such facilities, in addition to DRIBs, are SPIRAL1 in France and the accelerator at Louvain-la-Neuve (Belgium). However, the energy of the ${}^6\text{He}$ beam at Louvain-la-Neuve does not exceed 5 MeV/A.

1. EXPERIMENTAL METHOD

We used a beam of accelerated ${}^6\text{He}$ ions with an energy of up to 60 MeV. The ${}^6\text{He}$ beam was provided by the DRIBs complex at FLNR (JINR). This complex is a tandem including the FLNR cyclotrons U400M and U400 (Fig. 1). A ${}^7\text{Li}$ beam accelerated to 35 MeV/A at the U400M accelerator bombarded a thick beryllium target in which, as a result of the ${}^9\text{Be}({}^7\text{Li}, p)$ -reaction, ${}^6\text{He}$ nuclei were produced and implanted into a porous carbon stopper. This stopper was further heated to 1600° and ${}^6\text{He}$ could then diffuse into the ECR-source chamber. After ionization of the ${}^6\text{He}$ atoms in the ion source, the single-charged ${}^6\text{He}$ ions were transported to the second accelerator U400, where they were accelerated to an energy of about 60 MeV/A. The extraction of the ${}^6\text{He}^{+2}$ beam was achieved by a thin carbon stripping foil. The optimization and transport of the ${}^6\text{He}^{+2}$ -ion beam made it possible, without applying any additional collimation, to have a (7×7) -mm beam spot on the physical target, the beam energy being $E = 60.3$ MeV, the energy resolution ± 0.4 MeV and the intensity $5 \cdot 10^6$ pps, when the ${}^7\text{Li}$ -beam intensity was 600 pA (Fig. 2). For the beam diagnostics of the low-energy ${}^6\text{He}$ ions scintillator detectors were used [11] along the beam-transport line, whereas immediately in front of the physical setup the parameters of the beam (intensity and size) were measured with a specially designed multiwire proportional chamber [12]. The final energy of the beam was measured using the MSP-144 magnetic spectrometer [13].

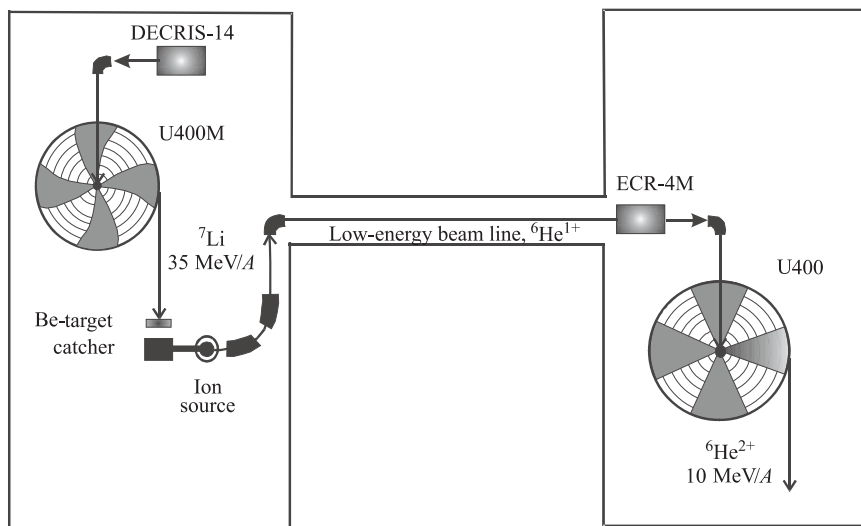


Fig. 1. Schematic layout of the DRIBs complex for producing the radioactive ${}^6\text{He}$ beam

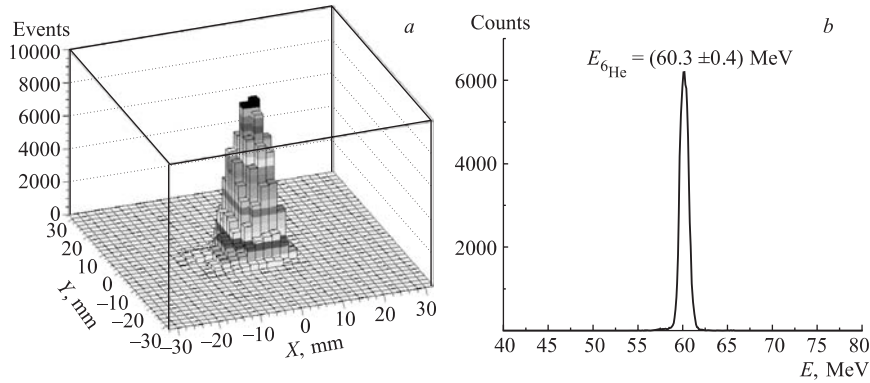


Fig. 2. Profile of the ${}^6\text{He}$ beam extracted from the U400 cyclotron (a) and its energy resolution (b)

Our aim was to study the interaction of ${}^6\text{He}$ with different target nuclei. In the present paper, results of measurements of the excitation functions for fusion and transfer reactions involving the accelerated ${}^6\text{He}$ ions are presented. The measurement of the yields of the products of the fusion reaction after the evaporation from the compound nucleus of x neutrons and of the transfer reactions was performed by the activation method. Two stacks of foils were placed in the reaction chamber of the magnetic spectrometer MSP-144 on the way of the ${}^6\text{He}$ beam: first — a stack of 13–50 μm thick gold foils, and further downstream a second stack of ${}^{206}\text{Pb}$ targets, 600–700 $\mu\text{g}/\text{cm}^2$ each (Fig. 3). In order to tune the ${}^6\text{He}$ beam and to measure its intensity and spatial distribution, the multiwire proportional chamber for beam diagnostics was placed in front of the stacks. After passing through the two stacks the beam entered the magnetic spectrometer MSP-144, which gave a precise measurement of the residual energy of the beam. The ${}^6\text{He}$ energy and the energy loss in each layer of the stacks was calculated with the LISE code [14] and the calculated residual energy was compared to the value measured by the magnetic spectrometer. In this way, in spite of the rather large energy dispersion of the beam at the end of the stacks (± 2 MeV), the absolute value of the energy was determined with good accuracy (not worse than 1 MeV).

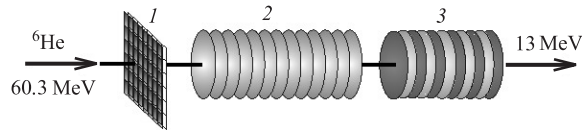


Fig. 3. Schematic layout of the activation experiments using the ${}^6\text{He}$ beam: 1 — multiwire proportional chamber, specially designed for beam diagnostics; 2 — stack of gold foils; 3 — stack of thin ${}^{206}\text{Pb}$ targets. The incident and final energies of the beam are also shown

After the irradiation the γ activity induced in the gold foils was measured off-line using HPGe detectors with high efficiency (about 10% for $E_\gamma = 662$ keV) and high energy resolution (1.5 keV for the γ transition at 1800 keV). Peaks in the γ spectra could be identified as belonging to the Tl isotopes, which are the decay products of the compound nucleus ${}^{203}\text{Tl}$

after the evaporation of 2–7 neutrons. The table contains the energies, half-lives and relative yields of the most intensive γ transitions in the corresponding fusion reaction decay products, which have been used for their identification.

Characteristics of the decay products of the compound nucleus ^{203}Tl

xn	Decay product	Half-life $T_{1/2}$, h	$E\gamma$, keV (I %)
2n	^{201}Tl	72.91	167.4 (10%)
3n	^{200}Tl	26.1	367.9 (87%)
4n	^{199}Tl	7.42	247.26 (9.3%)
5n	^{198}Tl	5.3	675.88 (11%), 587.2 (52%)
6n	^{197}Tl	2.84	152.2 (7.3%)
7n	^{196}Tl	1.84	344.9 (2%)

In addition to the Tl isotopes, γ transitions of the isotopes ^{196}Au , ^{198}Au and ^{199}Au could be identified in the spectra measured for the gold foils. The isotope ^{196}Au could be formed as a result of the stripping of one neutron, ^{198}Au and ^{199}Au — after the pickup of one and two neutrons, respectively, in the interaction of the ^6He beam with the ^{197}Au target nuclei.

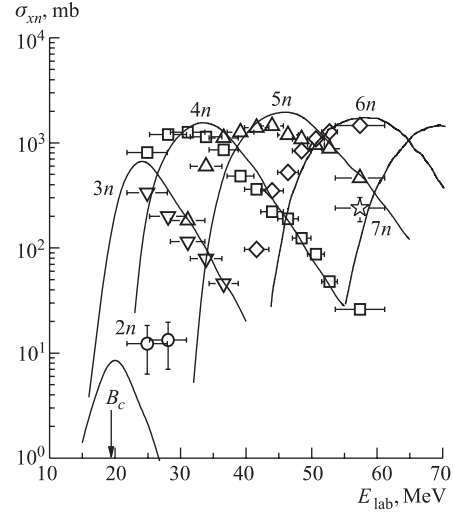
The ^{206}Pb stack was measured using an α spectrometer and the excitation function for the formation of the compound nucleus ^{212}Po and its decay by emission of two neutrons ($^{206}\text{Pb}(^6\text{He}, 2n)^{210}\text{Po}$) was obtained in the beam-energy range 13–24 MeV (the Coulomb barrier for the given reaction is 20 MeV). The ^{210}Po isotope was identified by the α -particle energy ($E_\alpha = 5.3$ MeV) and its half-life ($T_{1/2} = 138$ d). The energy resolution of the α spectrometer amounted to about 50 keV, and the total efficiency of registration of the α particles was about 50%.

2. RESULTS AND ANALYSIS

On the basis of the measured yields of the isotopes, formed after the evaporation from the compound nucleus ^{203}Tl of 2 to 7 neutrons, taking into account the ^6He beam intensity and the target thicknesses, we could determine the cross sections for the formation of the different isotopes and their dependence on the bombarding energy (the excitation functions). The same procedure was applied for ^{210}Po , which was formed in the $^{206}\text{Pb}(^6\text{He}, 2n)^{210}\text{Po}$ reaction.

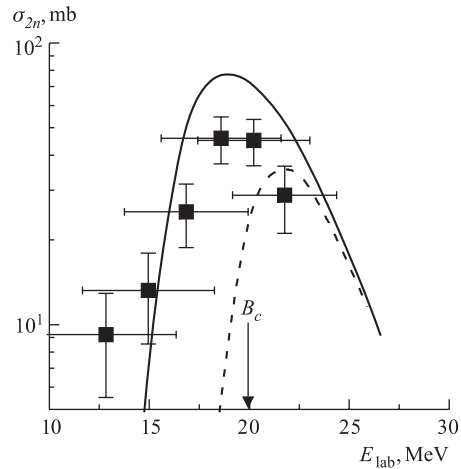
The excitation functions measured for the reaction channels $^6\text{He} + ^{197}\text{Au} \rightarrow ^{203-x}\text{Tl}$ are shown in Fig.4. The analysis of the obtained data was performed using the ALICE-MP code [15, 16]. The values of the parameters used were taken from analyses of experimental data on the cross sections of evaporation reaction channels induced by heavy ions in the range of medium and heavy nuclei. The solid curves in Fig.4 represent the results of the calculations. It can be seen that the experimental reaction cross sections are in agreement what concerns the maxima of the xn -channel distributions. The channel with the emission of two neutrons, in which the ^{201}Tl nucleus is produced, is not well described by the given model. As can be seen from the figure, the isotope ^{201}Tl is formed with a cross section larger than expected in the model. This may be connected with the fact that the reaction with total absorption of ^6He by the ^{197}Au target nucleus has a Q value equal to +12.2 MeV, which

Fig. 4. Experimental excitation functions for the ${}^{197}\text{Au} + {}^6\text{He} \rightarrow {}^{203-xn}\text{Tl}$ reaction, where $x = 2-7$. The symbols denote: \circ — $2n$, ∇ — $3n$, \square — $4n$, \triangle — $5n$, \diamond — $6n$, \star — $7n$ evaporation channels; the curves are the calculations with the ALICE-MP code [15,16] using the following parameters for the interaction potential: $r_0 = 1.29$ fm, $V = -67$ MeV and $d = 0.4$ fm. B_c is the Coulomb barrier for the ${}^6\text{He} + {}^{197}\text{Au}$ reaction



makes the reaction with the evaporation of two neutrons deeply subbarrier. The calculations, where fusion is described as the penetration of ${}^6\text{He}$ through the barrier, should result in decreased values of the cross sections. A similar situation arises for the ${}^{206}\text{Pb}({}^6\text{He}, 2n){}^{210}\text{Po}$ reaction (Fig. 5). However, in this case the reaction Q value is equal to $+4.2$ MeV, which must lead to somewhat larger cross-section values.

Fig. 5. Excitation function measured for the ${}^{206}\text{Pb}({}^6\text{He}, 2n){}^{210}\text{Po}$ reaction. \blacksquare — experimental values of cross sections for the formation of ${}^{210}\text{Po}$; dashed line — calculations within the framework of the statistical model; solid line — calculations using the two-step fusion model, taking into account the process of consecutive transfer of neutrons [17]. B_c is the Coulomb barrier



This difference is particularly well seen in Fig. 5, where the excitation function for the ${}^{206}\text{Pb}({}^6\text{He}, 2n){}^{210}\text{Po}$ reaction is shown. The cross section for this reaction at the maximum, according to the statistical model calculations (the dashed line), should be small, because the reaction takes place at energies below the Coulomb barrier and is strongly suppressed. But, as can be seen from the presented data, even at energies 7 MeV below the Coulomb barrier for the ${}^{206}\text{Pb} + {}^6\text{He}$ reaction, the cross section for formation of ${}^{210}\text{Po}$, i.e. for the evaporation from the compound nucleus of two neutrons, is rather large and amounts to ~ 10 mb. Thus, due to the observation of the reaction with the evaporation of two neutrons we could draw

the conclusion that a considerable enhancement of the cross section for the fusion of ${}^6\text{He}$ with the ${}^{197}\text{Au}$ and ${}^{206}\text{Pb}$ nuclei exists at energies close to the barrier. In the same figure, the results of the calculations of the two-step fusion process are also presented [17]. In this model it is assumed that a consecutive transfer of neutrons from the ${}^6\text{He}$ nucleus to the target nucleus takes place. In this case, the excitation energy of the nuclear system increases by $E_{\text{cm}} + Q_{qq}$, a value which is quite higher than the energy of the Coulomb barrier and leads to the tunneling, at the latest stage, of the α particle through the barrier.

The agreement between the experimental reaction cross sections for the ${}^{206}\text{Pb}({}^6\text{He}, 2n){}^{210}\text{Po}$ reaction and the calculated ones can be considered as evidence that the sequential fusion process for weakly bound nuclei seems to be the main process, which influences the fusion probability of ${}^6\text{He}$ with ${}^{206}\text{Pb}$ and leads to the increase in the reaction cross section at energies far below the barrier.

The cross sections for the evaporation residues in the ${}^{197}\text{Au}({}^6\text{He}, 2n){}^{201}\text{Tl}$ and ${}^{206}\text{Pb}({}^6\text{He}, 2n){}^{210}\text{Po}$ reactions are shown together in Fig. 6 as a function of the ratio of the ${}^6\text{He}$ energy in the center-of-mass system (E_{cm}) and the energy of the Coulomb barrier (B_c). Good agreement is observed between the experimental data for the $2n$ -evaporation channels in both reactions and the theoretical calculation assuming a sequential fusion mechanism.

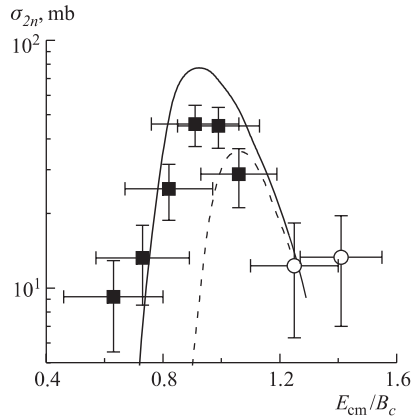


Fig. 6. Evaporation residue cross sections for the reactions ${}^{197}\text{Au}({}^6\text{He}, 2n){}^{201}\text{Tl}$ (\circ) and ${}^{206}\text{Pb}({}^6\text{He}, 2n){}^{210}\text{Po}$ (\blacksquare) as a function of the ratio of the center-of-mass ${}^6\text{He}$ energy and the Coulomb barrier (E_{cm}/B_c)

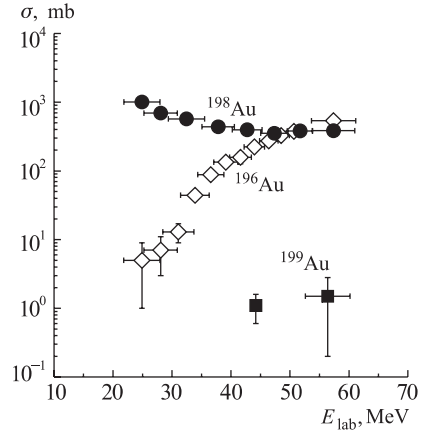


Fig. 7. Experimental excitation functions for the formation of the isotopes ${}^{196}\text{Au}$, ${}^{198}\text{Au}$ and ${}^{199}\text{Au}$ in the ${}^{197}\text{Au} + {}^6\text{He}$ reaction

The measured excitation functions for the formation of the gold isotopes ${}^{196}\text{Au}$, ${}^{198}\text{Au}$ and ${}^{199}\text{Au}$ in their ground states in the ${}^{197}\text{Au} + {}^6\text{He}$ reaction are shown in Fig. 7. From the obtained data it follows that close to the barrier the probability of formation of the ${}^{198}\text{Au}$ isotope is rather large ($\sigma \sim 1$ b). Unfortunately, in the present experiment we did not measure the cross section for the formation of ${}^{198}\text{Au}$ at energies lower than the barrier (~ 20 MeV). Meanwhile it seems, the increased formation probability of reaction products at energies close to the barrier, which imitate the transfer of one neutron to the target nucleus, can be used to explain the enhanced probability, formerly observed in [6, 7], of subbarrier fission in the ${}^{238}\text{U} + {}^6\text{He}$ reaction.

It should also be noted that in our experiment a relatively low yield was observed for the ${}^{199}\text{Au}$ isotope.

CONCLUSIONS

In the present paper we have presented the results of the first experiments performed at the accelerator complex DRIBs. We should once more mention that the ${}^6\text{He}$ beam intensity reached $\sim 5 \cdot 10^6$ pps. In the forthcoming experiments the beam intensity is supposed to reach 10^8 pps. Then we plan to measure in detail at energies close to the Coulomb barrier the behaviour of the excitation functions for the one- and two-neutron evaporation channels in the interaction of ${}^6\text{He}$ with ${}^{206}\text{Pb}$ and ${}^{197}\text{Au}$, as well as the excitation functions for the transfer of one and two neutrons and the total reaction cross section. Such measurements, we believe, can give a possibility to understand the mechanism of interaction of the ${}^6\text{He}$ nuclei with other nuclei at energies close to the Coulomb barrier.

Acknowledgements. Finally, the authors would like to express their gratitude to the accelerator crew headed by G.G. Gulbekian for the great effort to put into operation the accelerator complex DRIBs and to obtain the ${}^6\text{He}$ beam. We are also indebted to M.G. Itkis and S.N. Dmitriev for their support in performing this experiment, and to V.I. Zagrebaev for making available his calculations of the fusion reaction cross sections and for fruitful discussions.

The present investigation was carried out with the support of INTAS by grant No. 00-00463, RFBR by grant No. 04-02-17372, as well as by grants from the Czech Republic, Poland and Bulgaria in the framework of their collaboration with JINR.

REFERENCES

1. *Penionzhkevich Yu. E. et al. // Nucl. Phys. A. 1995. V. 588. P. 258; Fomichev A. S. et al. // Z. Phys. A. 1995. V. 351. P. 129.*
2. *Hussein M. S. et al. // Phys. Rev. C. 1992. V. 46. P. 377; Nucl. Phys. A. 1995. V. 588. P. 85c.*
3. *Dasso C. et al. // Nucl. Phys. A. 1996. V. 597. P. 473.*
4. *Stelson P. H. // Phys. Rev. C. 1990. V. 41. P. 1584.*
5. *Kolata J. J. et al. // Phys. Rev. Lett. 1998. V. 81, No. 21. P. 4580.*
6. *Trotta M. et al. // Phys. Rev. Lett. 2000. V. 84, No. 11. P. 2342.*
7. *Raabe R. et al. // Nature. 2004. V. 431. P. 823.*
8. *Pietro A. Di. et al. // Phys. Rev. C. 2004. V. 69. P. 044613.*
9. *Navin A. et al. // Ibid. V. 70. P. 044601.*
10. *Oganessian Yu. Ts., Gulbekian G. G. // Proc. of the Intern. Conf. «Nuclear Shells — 50 Years», Dubna, 1999 / Eds. Yu. Ts. Oganessian, W. von Oertzen, R. Kalpakchieva. Singapore, 2000. P. 61–75.*

46 *Penionzhkevich Yu. E. et al.*

11. *Kuznetsov V.D. et al.* FLNR Scientific Report 2001–2002 / Ed. A. G. Popeko. Dubna, 2003. P. 223; 224.
12. *Astabyan R. A. et al.* FLNR Scientific Report 2001–2002 / Ed. A. G. Popeko. Dubna, 2003. P. 212; FLNR Scientific Report 2003–2004 / Ed. A. G. Popeko. Dubna, 2005.
13. *Skobelev N. K. et al.* // Nucl. Instr. Meth. B. 2005. V. 227. P. 471.
14. <http://dnr080.jinr.ru/lise/>
15. *Muzychka Yu. A., Pustynnik B. I.* // Proc. of the Intern. School-Seminar on Heavy-Ion Physics, Alushta, 1983. Dubna, 1983. P. 420.
16. *Penionzhkevich Yu. E. et al.* // Phys. At. Nucl. 2002. V. 65, No. 9. P. 1563.
17. *Zagrebaev V. I.* // Phys. Rev. C. 2003. V. 67. P. 061601(R); Prog. Theor. Phys. Suppl. 2004. V. 154. P. 122.

Received on August 10, 2005.